



Prediction of energy injected into the grid using a hybrid artificial intelligence approach: case of the Ten Merina photovoltaic solar power plants (Senegal)

El Hadji Mbaye Ndiaye*, Alphousseyni Ndiaye, Mactar Faye, Mamadou Traoré, Daouda Gueye, Amadou Bâ

Research team energetic system and efficiency, Alioune Diop University of Bambey, BP 30 Senegal

Received: 29 April 2025 / Received in revised form: 14 June 2025 / Accepted: 26 June 2025

Abstract:

This paper presents a Hybrid Particle Swarm Adaptive Neuro Fuzzy Inference System (HPSANFIS) technique for predicting the energy injected into the grid by a photovoltaic (PV) power plant. In the proposed predicting model, Particle Swarm Optimization (PSO) was selected as the optimizer for the training process of the Adaptive Neuro Fuzzy Inference System (ANFIS). The proposed method is validated by using actual data from the Ten Merina solar power plants in Senegal. The artificial intelligence (AI) method is compared with methods based on the performance ratio (A1 method) and the method of the online simulation software Photovoltaic Geographical Information System. These methods were implemented on MATLAB/Simulink. A daily production prediction was made and analyzed according to the season (dry or rainy). The performance study showed Root Mean Square Error of 0.6823 kWh, 23.9178 kWh, and 133.0048 kWh, respectively, for the proposed model, A1, and Photovoltaic Geographical Information System models. This study also showed that the proposed model has the highest yield across all seasons.

Keywords: Prediction; PSO; HPSANFIS; Photovoltaic Geographical Information System; Artificial Intelligence; Solar power plant.

1 Introduction

Global economic conditions have not always been favorable during the year 2018, which, at the national level, was manifested by an average increase in the prices of fuels by 20% compared to 2017. The use of fossil fuels has an undesirable impact on the environment (greenhouse gas emissions and nuclear accidents). To overcome these

 $\label{lem:email$



^{*} Corresponding author:

problems, it is necessary to resort to renewable energies [1]. Solar Photovoltaic energy system is considered as one of the most promising technologies of renewable energy [2-5]. The use of Photovoltaic (PV) modules for electricity generation purposes has seen the greatest improvement in the world in recent decades [6-8]. In Senegal, persistent production deficits have driven the state to adopt renewable energy sources such as solar and wind power. Solar energy is abundant in Senegal, with an overall horizontal sunshine level greater than 2000 kWh/m²/year and more than kW/m²/year of direct radiation and an average global radiation of 5.8 kW/m²/day [9]. In 2018, solar PV represented 11.45% with a total installed power of 143 MWp [10].

Predicting the energy of PV systems is a challenging task, as it depends on irradiation and other weather parameters. It allows optimal management of the solar power plant but also of the grid. This will boost the use of renewable energy and make a significant contribution to the energy transition.

Predicting the output of solar PV power is a critical issue. In the existing literature, solar power prediction has been widely studied [4, 11, 12]. Short-term power prediction methods for solar power plants primarily comprise two classes: physical methods and statistical methods. Physical methods imply that a physical equation is established for prediction, rendering of the solar power generation procedure and system characteristics, and in combination with forecast weather data. In [13], the authors used a physical method based on the Kalman filter to study the impact of meteorological parameters on short-term forecasting. In [14], an analysis of different techniques for an accurate estimation of the wind effects of PV is carried out. The authors tested several existing methods to evaluate the PV module temperature as a function of solar irradiance, ambient temperature, and wind.

Statistical methods are intended summarize inherent laws to predict solar power based on historical power data [15]. Statistical methods have been used successfully in time series forecasting for several decades. Using the statistical approach, the relations between predictors, variables used as an input into the statistical method, and the variables to be predicted are derived from statistical analysis [16]. In [17], the authors made very short-term power predictions for PV power plants using a simple and effective statistical method. This method, based on short-term multivariate historical datasets, is a combination of radiation classification coordinate (RCC) and long short-term memory (LSTM).

The above methods have their respective advantages, but the non-stationary characteristics of solar power output have a significant effect on the convergence and properties of them. A few studies have been conducted to predict the output of solar PV systems.

In recent years, artificial intelligence (AI) methods have proven to be a powerful tool for nonlinear complex engineering applications. The main advantages of these computational tools are their versatility, robustness, fast computing processes, and optimization achieved through learning processes [2, 12, 18].

In [15], a comprehensive method to predict the solar power output based on historical data is presented. The work explores the option of using Artificial Intelligence-based methods like Artificial Neural Networks (ANN) and an Adaptive Neuro-Fuzzy Inference System (ANFIS) for predicting the power output. It can be inferred from the results that, regarding predicting PV generation, the ANN-based forecast delivers better results when compared to the NF-based forecast. ANN is used in [19] to estimate the Performance Ratio (PR) of PV modules under outdoor operating conditions. The results have shown that ANN accurately method the PR regardless of PV module technology. Bassam et al. [18] use an ANFIS method with seven input parameters to estimate PV array operating temperature. Validation results indicate that the ANFIS method generates good temperature estimation for the PV array at different atmospheric and operational conditions. A method based on ANN is presented in [20] for predicting solar irradiance. In [21], a short-term forecasting for solar irradiation is presented. This methodology is based on the multilayer Neural Network. The results show the efficiency of this method and the relevance of the chosen approach. In [12] a comparison of different soft computing techniques for forecasting energy production is presented. These techniques based on Data Mining (DM) are ANN, Support Vector Machines (SVM) and Decision Trees (DT). In [22], the authors proposed a prediction technique based on ANFIS optimized by Genetic Algorithm (GA) and Particle Swarm Optimization (PSO) (GA-PSO-ANFIS) for short-term photovoltaic power generation forecasting. In [23], the power output forecasting of PV systems by using ANFIS, comparing the accuracy with particle swarm optimization combined with the artificial neural network method (PSO-ANN) is simulated. The simulation results show that the forecasting with the ANFIS methodology is more accurate than the PSO-ANN method.

All these techniques have limitations ranging from robustness to implementation complexity. In addition, artificial intelligence techniques are most suitable for solar PV systems where a medium-term horizon (H 24) is chosen. Among the techniques presented in this review of the literature, the ANFIS methodology is the most efficient for prediction. Like the other methods, this one presents a difficulty linked to the choice of its membership functions (MsF) (number and type) for its learning. This choice has a considerable impact on the performance of the algorithm and must, therefore, be made with precision. A large number of MsF implies the need to set additional parameters, thereby increasing the execution time of the algorithm. A very small number of MsF causes the algorithm to diverge due to a lack of information.

The contribution of this study is to develop a Hybrid Particle Swarm Adaptive Neuro Fuzzy Inference System (HPSANFIS) algorithm for the prediction of the daily production of a photovoltaic solar power plant to improve plant planning and reduce certain risks. The rest of this paper is organized as follows: the second section describes the study site and data presentation. The third section presents the proposed approach. The fourth section presents the obtained results, and the last section contains the conclusions.

2 Study site and data presentation

The study site is Ten Merina solar power plants located at 15°9'21.1"N and 16°35'40.2"W in Senegal in West Africa (Fig.1). This solar power plant is connected to the grid of the national society of electricity (SENELEC).

The Ten Merina solar power plant has a capacity of 29.5 MWp. It delivers 20 MW $\operatorname{national}$ electrical grid the SENELEC. This solar power plant avoids the emission of 34 kT of CO₂ per year. The specific characteristics of the site area are given in Table 1. A data acquisition system records the evolution of the operating parameters measured by the inverters. Two types of measurements are recorded: measures to control the facility's production (production history) and measures to facilitate maintenance (real-time measurements and fault history). The real time and cumulative values can be viewed locally via a serial link or remotely via an integrated modem connection. The recorded information is automatically returned and managed as synoptic and detailed in understandable tables. This system is a full SCADA (Supervision, Control & Data Acquisition)

which allows the operator to virtually control the operation of the plant remotely. The data acquisition system allows, among other parameters, to track irradiation, potential produced power, photovoltaic module temperatures, ...

In this work, we use solar irradiation data, photovoltaic module temperatures, and production data. The data series ranges from February 2, 2018, to August 18, 2018, which is the time of year when production is most critical. Usually, during this period, it is very hot with considerable dust. The period from February 2nd to August 18, 2018, coincides with the height of Senegal's hot season, characterized by intense solar irradiation, high module temperatures, frequent dust events, and marked transitions between the dry and rainy seasons. Production during this window is most susceptible to extreme climatic variations and operational challenges, including rapid weather fluctuations and maintenance constraints. This makes the dataset particularly relevant to evaluating model performance under operationally challenging and variable conditions.

Table 1
The specific characteristics of the power plant.

Facility	
Output power	29.4912 MWp STC
Modules	
Type	CS: MAXPOWER CS6U-320-P JS: JKM320PP-72-320
Unitary power	Average of 320 Wp @STC
Number of modules	92160
Type of cell	Crystalline-polysilicium, 6 inch
Number of cells	72
Inverters	
Constructor	Schneider
Type	Conext Core XC-680
Number of inverters	36[12 PTR]
Unitary power	2040 KVA (3*680 KVA)
Site	
Site area	83 ha
Altitude	40 m

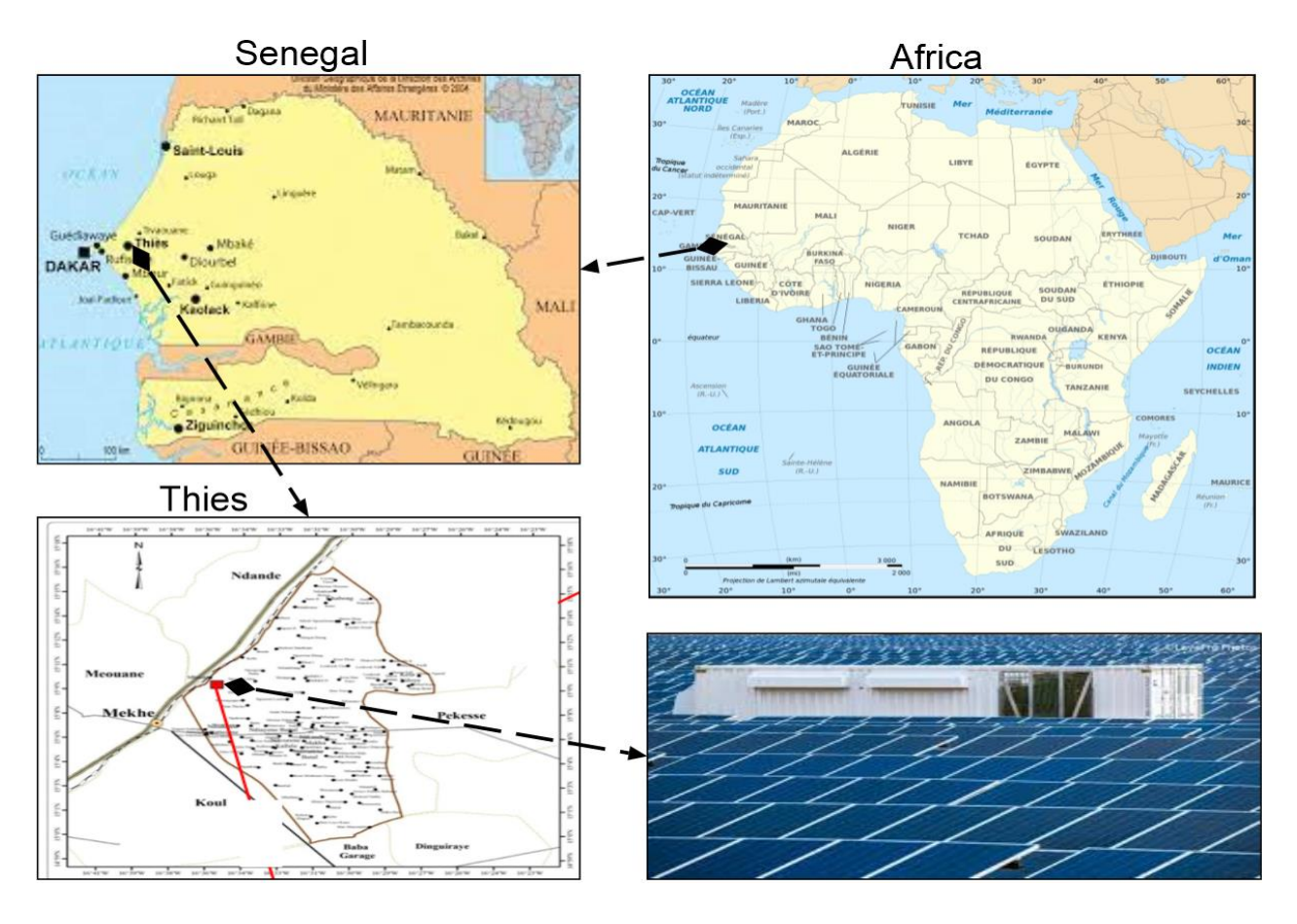


Fig. 1. Ten Merina solar power plant location

3 Materials and methods

Three methods are used in this work. Two analytics methods based on mathematical methods and a method based on artificial intelligence.

3.1 Analytic method based on the Performance ratio (A1 method)

A1 is an analytical method presented in the literature for predicting the output of a solar PV plant. It is based on the performance ratio.

Like any energy conversion system, the performance of a photovoltaic installation is characterized by its yield. It is the calculation of the Performance Ratio (PR) that makes it possible to account for the quality of operation of an installation independently of the irradiation or the peak power of the modules.

In this method, an estimate of the energy produced by the solar power plant is made based on the PR of the plant and the solar radiation measured during the same technical unavailability period, using the formula of Eq. (1).

$$Ep = \frac{PR*P_p*I_r}{I_{r,STC}} \tag{1}$$

Where E is electrical energy, which should, in theory, have been produced (kWh); PR is the average performance ratio during the reference periods; P_p is the actual nameplate capacity installed in the Facility (W); $I_{r,STC}$ is the standard solar radiation (Wh/m²); I_r is the solar radiation measured during the incident (kWh/m²).

The developed prediction method has two inputs: solar radiation and a performance ratio. The output is energy (Fig.2).

3.2 Photovoltaic Geographical Information System (PVGIS) method

PVGIS is a tool for estimating the production of grid-connected photovoltaic systems. Using its integrated Google Maps interface, it is very easy to obtain the production data of a PV system from the precise sunshine data of the site (including remote masks linked to relief, hills, and mountains). In addition, PVGIS offers precise, high-definition maps of sunshine

(irradiation in kWh/m²) and temperature for most countries in the world.

The PVGIS methodology is based on the irradiation and the yield of the installation. The energy is obtained by using Eq. (2).

$$E = A * I_r * C_p * r \tag{2}$$

Where A is the area of the installation; C_p is the coefficient of losses, and r is the plant efficiency.

The loss coefficient is evaluated over the entire installation. Losses are generally attributed to factors such as inverters, cables, ambient temperature, and irradiation level, among others.

This method incorporates two input variables: efficiency and solar irradiation. The output will give the energy (Fig. 3).

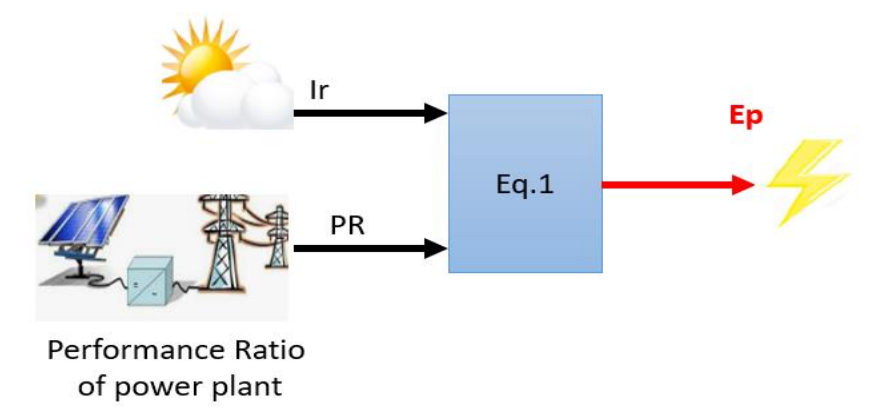


Fig.2. A1 method.

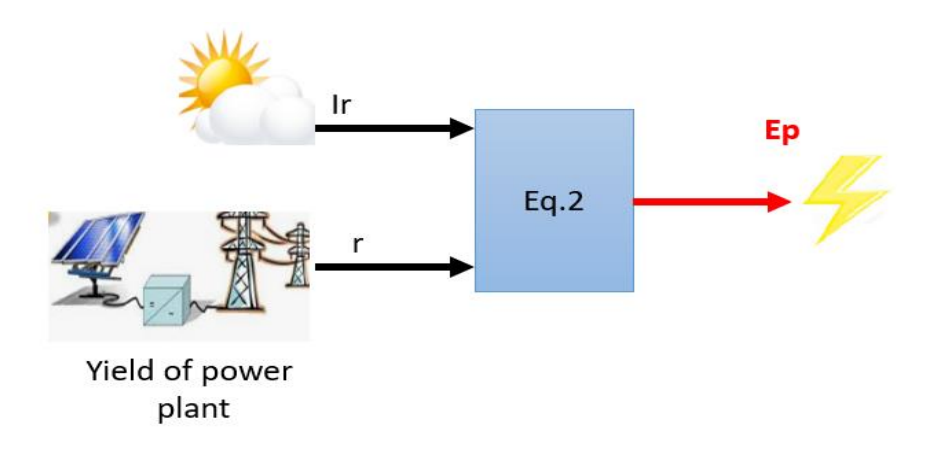


Fig.3. PVGIS method.

3.3 HPSANFIS method

The Adaptive Neuro-Fuzzy Inference System is a process for the mapping of a given data set from multiple inputs or a single input to a single output, which is achieved by fuzzy logic and artificial neural networks. The Neuro-Fuzzy (NF) system corresponds to a fuzzy method of Takagi-Sugeno, where the weights of the neural network are equivalent to the parameters of the fuzzy system. This structure was first presented by Jang in 1995 [24]. NF constructs a Fuzzy Inference System (FIS) whose fuzzy membership function parameters are adjusted using a hybrid learning method that includes back propagation and least square algorithms [25, 26]. NF comprises the advantages of ANN and FLC algorithms and can handle the non-linear behavior[27]. It provides a rapid dynamic response, high convergence speed, and a robust, flexible design. The NF produces a set of inference fuzzy rules to adjust the assigned membership function until the error is reduced and the desired output is obtained. The value of the membership function is adjusted until the error is minimized. It becomes a learning method and works to predict the production when the membership functions are adjusted. Moreover, the checking data is compared with the trained data. If an error is generated, the value of the membership function is adjusted until the error becomes minimum [28]. The membership functions are optimized and tuned by the application of back propagation and the least squares algorithm. To overcome this problem, optimization algorithms of the Meta-heuristic type are often used. Among them, we can cite the PSO. It is a stochastic, population-based evolutionary algorithm search

method, modeled after the behavior of bird flocks. The PSO algorithm maintains a swarm of individuals (called particles), where each particle represents a candidate solution. Particles follow a simple behavior: emulate the success of neighboring particles and their own achieved successes. The position of a particle, therefore, is influenced by the best particle in a neighborhood as well as the best solution found by all the particles in the entire population [29-32]. Each particle represents a potential solution in the swarm and determines the required parameters that minimize the objective function in a given search space. The personal best position P_{bes} corresponds to the position in the search space where the particle has the largest value as determined by the objective function "F", considering a minimization problem. The global best position is the highest position value amongst all the personal bests, which is denoted by G_{best} [29, 33]. Here, a Hybrid HPSANFIS-based algorithm is proposed for optimal tuning of NF membership function. One of the biggest difficulties with NF is the optimal choice of membership functions (MsF). This means that, in general, the output obtained differs from that desired and which is materialized by the Root Mean Square Error (RMSE criterion). The HPSANFIS flowchart is shown in Fig. 2. Its structure includes two inputs (Solar Irradiation and PV module Temperatures) and one output (Production) (Fig.4). The MsF function represents the activation function of the neurons in the first layer. It can be in several forms (Triangle, Trapezoidal, Gaussian, ...). Eq. 3 presents a membership function (for the inputs) of the type. PSO algorithm Gaussian implemented assuming PSO parameters as indicated in Table 2.

Table 2 Parameters used for PSO algorithm.

Parameters	Values
Number of particles	25
Number of iterations	1000
Maximum velocity	0.1*50
Acceleration constant 1	1
Acceleration constant 2	2
Inertia weight	1
Inertia weight damping ratio	0.99

Each controller variable is defined by 10 MsF. The speech universe of each ANFIS controller variable is divided into 10 MsF defined by their center. ANFIS has a fixed structure composed of five layers (Fig.5). They are modeled by Eqs. (3) to (10).

Layer 1: Fuzzification

Layer 1: Fuzzification
$$\begin{cases}
\mu_{Ai}(I_r) = exp \left[-\left(\frac{l_{ri} - \bar{l}_r}{\sigma(I_{ri})}\right)^2 \right] \\
\mu_{Bi}(T_m) = exp \left[-\left(\frac{T_{mi} - \bar{T}_m}{\sigma(T_{mi})}\right)^2 \right]
\end{cases} (3)$$

$$\begin{cases}
\bar{l}_r = \frac{1}{N} \sum_{i=1}^{N} l_{ri} \\
\bar{T}_m = \frac{1}{N} \sum_{i=1}^{N} T_{mi}
\end{cases} (4)$$

$$\begin{cases}
x = \frac{1}{N} \sum_{i=1}^{N} (l_{ri} - \bar{l}_r) \\
y = \frac{1}{N} \sum_{i=1}^{N} (T_{mi} - \bar{T}_m)
\end{cases} (5)$$

$$\begin{cases}
\sigma(l_{ri}) = \sqrt{x} \\
\sigma(T_{mi}) = \sqrt{y}
\end{cases} (6)$$

$$\begin{cases} \bar{I}_r = \frac{1}{N} \sum_{i=1}^{N} I_{ri} \\ \bar{T}_m = \frac{1}{N} \sum_{i=1}^{N} T_{mi} \end{cases}$$
 (4)

$$\begin{cases} x = \frac{1}{N} \sum_{i=1}^{N} (I_{ri} - \bar{I}_r) \\ y = \frac{1}{N} \sum_{i=1}^{N} (T_{mi} - \bar{T}_m) \end{cases}$$
 (5)

$$\begin{cases} \sigma(I_{ri}) = \sqrt{x} \\ \sigma(T_{mi}) = \sqrt{y} \end{cases}$$
 (6)

where μ is the Gaussian MsF; x and y are variances; σ is the Standard deviation; \bar{I}_r is the average of the irradiation; \bar{T}_m is the average module temperature; N is the size of the database.

Layer 2: Fuzzy rules

$$w_{i} = \mu_{Ai}(I_{r}) * \mu_{Bi}(T_{m}) = \exp\left[-\left(\frac{I_{ri} - \bar{I}_{r}}{\sigma(I_{ri})}\right)^{2} - \left(\frac{T_{mi} - \bar{T}_{m}}{\sigma(T_{mi})}\right)^{2}\right]$$
(7)

where w_i is the degree of activation of fuzzy rules.

Layer 3: Normalization

$$\overline{w}_{i} = \frac{w_{i}}{\Sigma_{i} w_{i}} = \frac{\exp\left[-\left(\frac{l_{ri} - \overline{l}_{r}}{\sigma(l_{r})}\right)^{2} - \left(\frac{T_{mi} - \overline{T}_{m}}{\sigma(T_{m})}\right)^{2}\right]}{\Sigma_{i} \exp\left[-\left(\frac{l_{ri} - \overline{l}_{r}}{\sigma(l_{ri})}\right)^{2} - \left(\frac{T_{mi} - \overline{T}_{m}}{\sigma(T_{mi})}\right)^{2}\right]} \quad (8)$$

where \overline{w}_i is the degree of veracity of the activation of a neuron.

Layer 4: Defuzzification

$$G_i = \overline{w}_i * E_{ai} = \frac{\exp\left[-\left(\frac{I_{ri} - \overline{I}_r}{\sigma(I_r)}\right)^2 - \left(\frac{T_{mi} - \overline{T}_m}{\sigma(T_m)}\right)^2\right]}{\sum_i \exp\left[-\left(\frac{I_{ri} - \overline{I}_r}{\sigma(I_{ri})}\right)^2 - \left(\frac{T_{mi} - \overline{T}_m}{\sigma(T_{mi})}\right)^2\right]} \times$$

$$(p_i * I_r + q_i * T_m + r_i) \tag{9}$$

where $E_{ai} = (p_i * I_r + q_i * T_m + r_i)$ is the actual production of the power plant; (pi, qi, ri) are output parameters (consequents), determined during the learning process; G_i is the output of the fourth layer.

Layer 5: Output

$$\begin{split} E_{p} &= \sum_{i} \overline{w}_{i} * E_{ai} \\ &= \sum_{i} \left\{ \frac{\exp\left[-\left(\frac{l_{ri} - \overline{l}_{r}}{\sigma(l_{r})}\right)^{2} - \left(\frac{T_{mi} - \overline{T}_{m}}{\sigma(T_{m})}\right)^{2}\right]}{\sum_{i} \exp\left[-\left(\frac{l_{ri} - \overline{l}_{r}}{\sigma(l_{ri})}\right)^{2} - \left(\frac{T_{mi} - \overline{T}_{m}}{\sigma(T_{mi})}\right)^{2}\right]} \times (p_{i} * \\ I_{r} + q_{i} * T_{m} + r_{i}) \right\} \end{split} \tag{10}$$

where Ep is the Predicted production (Pr). The consequent parameters are given in Table 3

Table 3 Consequent parameters of HPSANFIS

MsF pi qi ri MsF1 -2.53 -512.77 36808.90 MsF2 20.40 -571.49 38572.09 MsF3 17.44 -244.77 35776.15 MsF4 15.26 -517.38 33502.09 MsF5 21.42 -529.03 35849.30 MsF6 33.31 -487.14 48511.01 MsF7 18.81 -1585.20 -387855.60 MsF8 11.60 -951.17 -163653.02 MsF9 20.12 -466.60 36407.45 MsF10 22.81 -719.93 30265.01				
MsF2 20.40 -571.49 38572.09 MsF3 17.44 -244.77 35776.15 MsF4 15.26 -517.38 33502.09 MsF5 21.42 -529.03 35849.30 MsF6 33.31 -487.14 48511.01 MsF7 18.81 -1585.20 -387855.60 MsF8 11.60 -951.17 -163653.02 MsF9 20.12 -466.60 36407.45	MsF	pi	qi	ri
MsF3 17.44 -244.77 35776.15 MsF4 15.26 -517.38 33502.09 MsF5 21.42 -529.03 35849.30 MsF6 33.31 -487.14 48511.01 MsF7 18.81 -1585.20 -387855.60 MsF8 11.60 -951.17 -163653.02 MsF9 20.12 -466.60 36407.45	MsF1	-2.53	-512.77	36808.90
MsF4 15.26 -517.38 33502.09 MsF5 21.42 -529.03 35849.30 MsF6 33.31 -487.14 48511.01 MsF7 18.81 -1585.20 -387855.60 MsF8 11.60 -951.17 -163653.02 MsF9 20.12 -466.60 36407.45	MsF2	20.40	-571.49	38572.09
MsF5 21.42 -529.03 35849.30 MsF6 33.31 -487.14 48511.01 MsF7 18.81 -1585.20 -387855.60 MsF8 11.60 -951.17 -163653.02 MsF9 20.12 -466.60 36407.45	MsF3	17.44	-244.77	35776.15
MsF6 33.31 -487.14 48511.01 MsF7 18.81 -1585.20 -387855.60 MsF8 11.60 -951.17 -163653.02 MsF9 20.12 -466.60 36407.45	MsF4	15.26	-517.38	33502.09
MsF7 18.81 -1585.20 -387855.60 MsF8 11.60 -951.17 -163653.02 MsF9 20.12 -466.60 36407.45	MsF5	21.42	-529.03	35849.30
MsF8 11.60 -951.17 -163653.02 MsF9 20.12 -466.60 36407.45	MsF6	33.31	-487.14	48511.01
MsF9 20.12 -466.60 36407.45	MsF7	18.81	-1585.20	-387855.60
11010 20112 100100 00101110	MsF8	11.60	-951.17	-163653.02
MsF10 22.81 -719.93 30265.01	MsF9	20.12	-466.60	36407.45
	MsF10	22.81	-719.93	30265.01

The error between actual and predicted production is minimized with the objective function F (Eq. (11)), which should be minimized. The best position discovered by any particle in the entire swarm is the best global position.

$$F = \int (p_i * I_r + q_i * T_m + r_i) - \sum_i \left\{ \frac{\exp\left[-\left(\frac{I_{ri} - \overline{I}_r}{\sigma(I_{ri})}\right)^2 - \left(\frac{T_{mi} - \overline{T}_m}{\sigma(T_{mi})}\right)^2\right]}{\sum_i \exp\left[-\left(\frac{I_{ri} - \overline{I}_r}{\sigma(I_{ri})}\right)^2 - \left(\frac{T_{mi} - \overline{T}_m}{\sigma(T_{mi})}\right)^2\right]} * (p_i * I_r + q_i * T_m + r_i) \right\}$$

$$(11)$$

Eq. (11) shows that optimizing the fitness function means optimizing the parameters $(p,q,r,and \sigma)$. The particles Gbest and *Pbesti* are saved by taking up the objective function's values during the optimization process. The next velocity (Eq. (13)) and position (Eq. (12)) of the candidate solution are determined by the basic PSO algorithm. The best position reached by the swarm is modeled by Eq. (14). Particles are represented by MsF.

$$\begin{cases} \mu(I_r)_i^{t+1} = \mu(I_r)_i^t + \left(\frac{d\mu(I_r)}{dt}\right)_i^{t+1} \\ \mu(T_m)_i^{t+1} = \mu(T_m)_i^t + \left(\frac{d\mu(T_m)}{dt}\right)_i^{t+1} \end{cases}$$
(12)

$$\begin{cases} \left(\frac{d\mu(I_r)}{dt}\right)_i^{t+1} = w_c \left(\frac{d\mu(I_r)}{dt}\right)_i^t + c_1 r_{n1} P_{best,i} + c_2 r_{n2} G_{best} \\ \left(\frac{d\mu(T_m)}{dt}\right)_i^{t+1} = w_c \left(\frac{d\mu(T_m)}{dt}\right)_i^t + c_1 r_{n1} P_{best,i} + c_2 r_{n2} G_{best} \end{cases}$$
(13)

$$G_{best} = max \big(P_{best,i} \big) = \max(\mu(I_r)_i^t, \mu(T_m)_i^t) \big(14)$$

where P_{best} is the Personal best position for the particle itself; G_{best} is the Global best position among all particles; w_c is the Coefficient of inertia; c_1 and c_2 are acceleration coefficients; r_{n1} and r_{n2} are random numbers drawn uniformly in [0,1]. The same process applies to the temperature MsF (second input). Fig. 4 illustrates a flowchart of the methodology employed. The experimental database consists of

datasets measured during the Ten Merina plant system operations solar power between February 2, 2018, and August 18, 2018. Variables that integrate the database are solar irradiation, PV module temperature, and energy production. The ANFIS structure is generated from the two input variables to yield the optimum method for production prediction of the solar power plant. The inference system type is defined for the output method behavior, where a zero-order Sugeno method was employed in the modeling process due to the non-linear relation between inputs and the output method predictor. Thereby, the evaluation of several combinations of membership functions in the zero-order Sugeno ANFIS structure was suggested as a suitable strategy to find the optimum modeling the results. Conversely, membership function number corresponding to each input variable is optimized by PSO algorithm, where particles are materialized by birds. To validate the obtained results from the proposed predictor method, they were compared to the actual data, considering the statistical agreement. The root mean square error (RMSE) determines the accuracy of the method by comparing the deviation of simulated and experimental values. Knowledge of this criterion is relevant to evaluate whether the prediction sub-estimated or over-estimated with respect to real data. For methodological rigor, the dataset was partitioned as follows: 70% of the data (February 2nd to June 15, 2018) was used for training the HPSANFIS model, and 30% (June 16th to August 18, 2018) for testing. This stratified split ensures that the test set covers the onset and peak of the rainy season, allowing for robust assessment of generalizations over seasonal shifts.

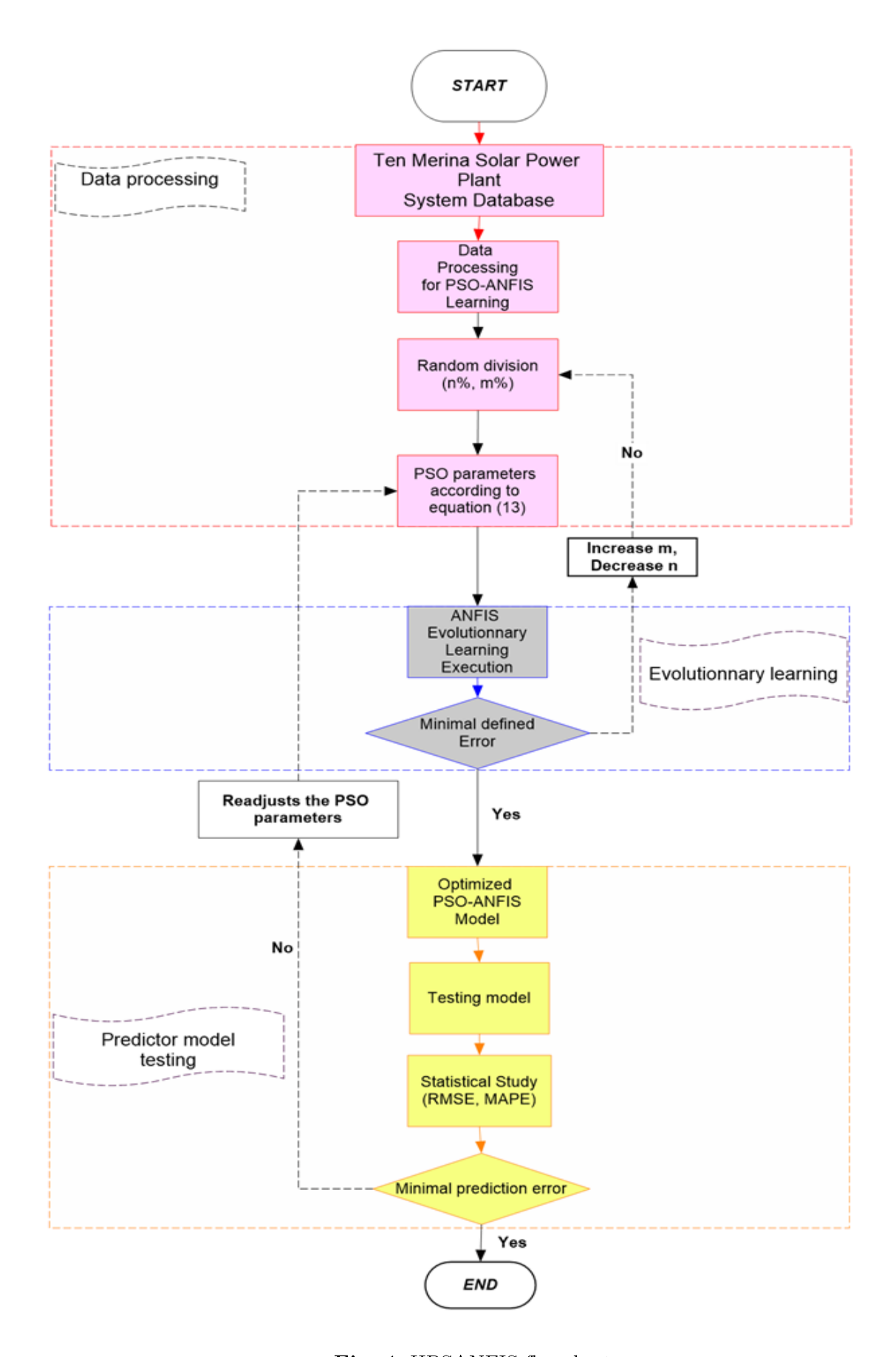


Fig. 4. HPSANFIS flowchart.

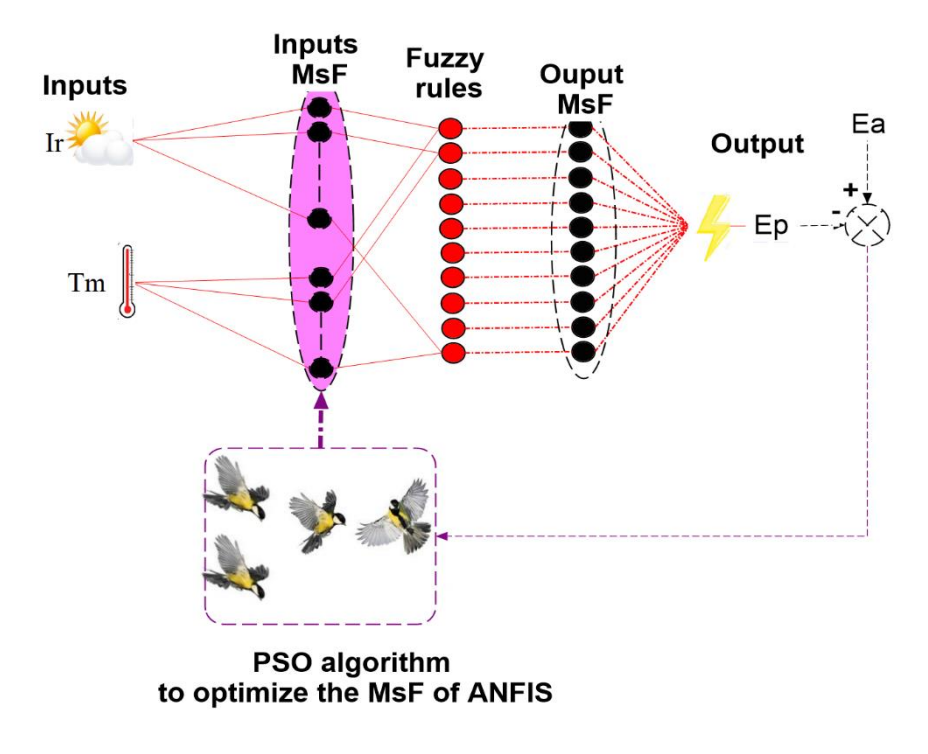


Fig. 5. HPSANFIS structure.

4 Results and discussion

This section presents the results of the yields and performance metrics obtained. Each of the three prediction methods has different inputs from the others.

4.1 Input parameters of prediction methods

The three prediction methods presented in this work each incorporate two inputs. These input parameters are all related to energy. The yield and performance ratio used in the PVGIS and A1 methods depend on climatic conditions such as temperature and irradiation. The yield is related to the PV field, while the performance ratio is evaluated over the entire installation. The reference period in this work is one day. These parameters are given in figure 6.

4.2 Learning of the HPSANFIS prediction method

Learning of the ANFIS methodology is accomplished through a series of epochs, performing an optimization process to minimize the differences between experimental data and simulated output. In this work, we carried out evolutionary learning with the PSO technique. PSO made it possible to make an optimal choice of the parameters of the MsF, but also the sharing of the database for the learning part and the test part. A comparative study is also carried out with a prediction method based on the ANFIS technique. Figure 7-a and 7-b show respectively train and test data with RMSE criteria (Eq. (15)). Table 4 gives the variation of specification parameters, and Table 5 gives the HPSANFIS learning parameters.

$$RMSE = \sqrt{\frac{1}{n}\sum_{i=1}^{n}(Output - Target)^{2}} \ (15)$$

The HPSANFIS prediction method generates the production from input data from solar irradiation $(Wh/m^2/day)$ and PV module temperatures (°C).

4.3 Comparative study of the three methods

Fig. 8 shows the variation in predicted production with the different methods. This production is compared with the actual daily production of the plant. As the A1 and PVGIS methods are classical, they do not adapt quickly to a large variation such as the one observed on March 10. On the other hand, the intelligent HPSANFIS

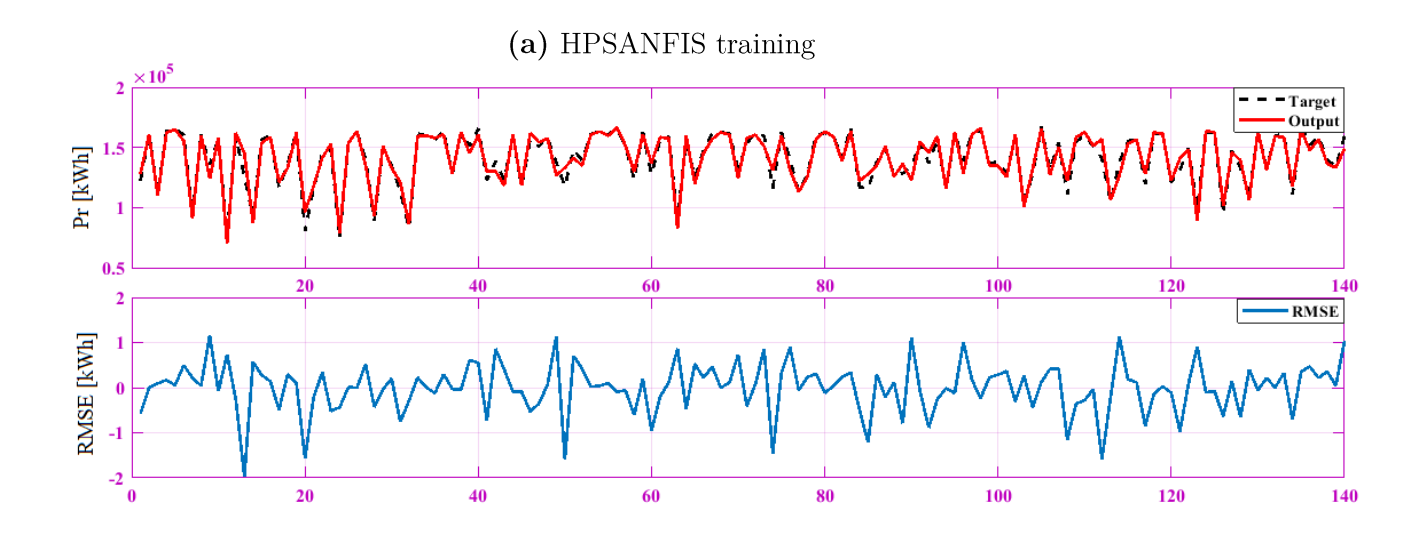
method follows the reference and predicts production during this period. This adaptive capacity is because, during a variation, the algorithm reevaluates its parameters relatively quickly thanks to its interprettation capacity. The same phenomenon is observed between June and August. The difference between the three methods in relation to the reference appears clearer. These results show that the adaptive method HPSANFIS is more efficient. The choice of prediction tools must take into account not only the method to be used, but also the inputs. As the output of the PV solar power plant is directly dependent on the module temperature and the solar irradiation, the prediction method must integrate the latter two.

Table 4
Prediction method parameters variation.

Parameters	Min	Max	Units
Irradiation (Ir)	3274.8	7874.7	$\mathrm{Wh}/\mathrm{m}^2/\mathrm{day}$
PV module Temperature (Tm)	29.800	59.000	$^{\circ}\mathrm{C}$
Production (Pr)	906.00	167860	kWh

Table 5
HPSANFIS learning parameters.

FIS type	Sugeno			
Epochs	1000			
Fuzzy Rules	10			
Input 1				
Membership functions				
Type	Gaussian			
Number	10			
Input 2				
Membership functions				
Type	Gaussian			
Number	10			
Output				
Mer	mbership functions			
Type	Linear			
Number	10			



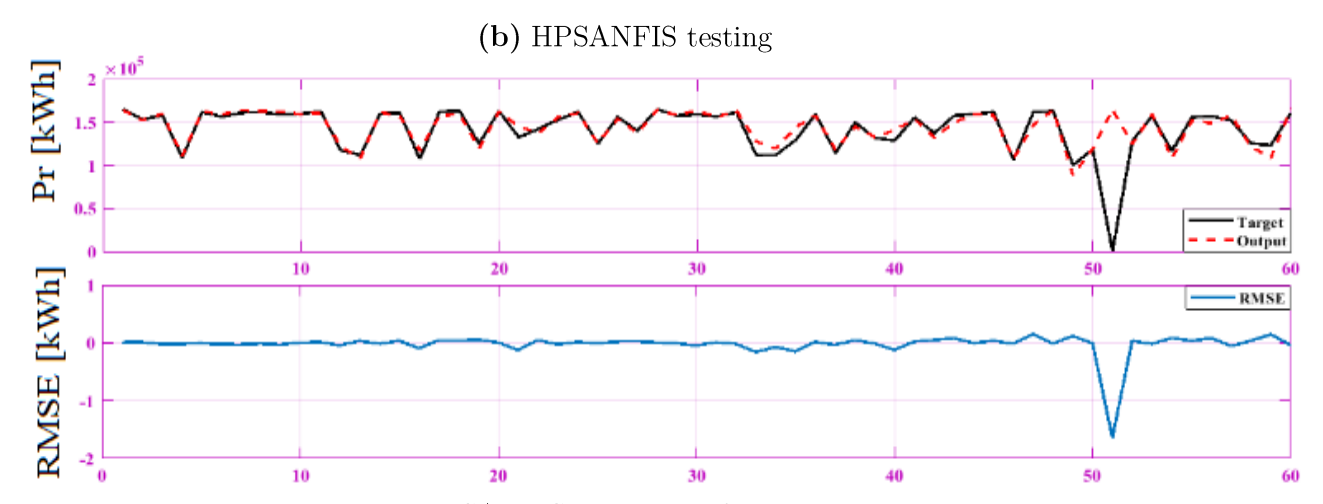


Fig. 7. HPSANFIS training and testing process.

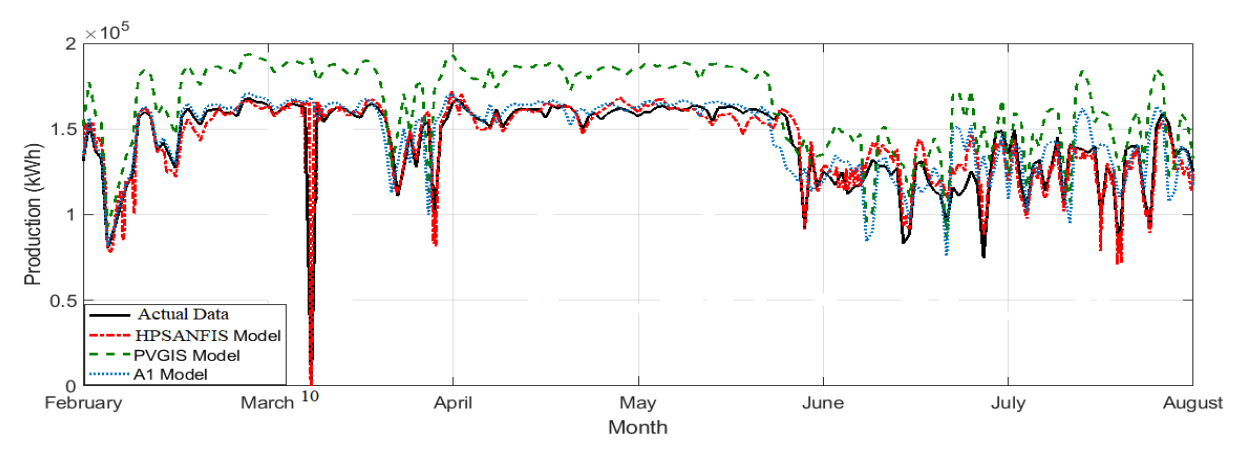


Fig. 8. Predicted production with HPSANFIS, PVGIS and A1 methods.

4.4 Impact of precipitation

In Senegal, there are two seasons: the dry season from November to June and the rainy season from June to October. Fig. 9 shows the evolution of wind speed, relative humidity, and precipitation. The relative humidity varies according to these seasons. In the area where the Ten Merina solar power plant is located, where high wind speeds are recorded (up to 7.5 m/s), an analysis of the production is carried out. It is noted that production is generally lower during the period of 26 June (rainy season). This is explained by the fact that the relative humidity is higher during this period, with a maximum value of 72.22%. In addition to this, there are also cloudy periods on rainy days. This significantly reduces production.

Fig. 10 shows the power plant's production during the dry season between February and June. This season consists of two periods. A period from February to April marked by strong winds (4 to 7.5 m/s), with very high temperatures reaching 39°C. Irradiation is generally good during this period except for a few cloudy days at the beginning of February and at the end of March. The period between April and June records the best irradiation rate of the year with average temperatures of 30 °C between May and June. On the other hand, relative humidity and wind speed are always high. All these factors have caused production to fluctuate during this period. The HPSANFIS method, therefore, enables to predict production inthese circumstances, unlike the othertwo methods, which are static in nature.

Fig. 13 shows the production of the plant during the rainy season between June and

During this season, the lowest August. wind speeds and the highest relative humidity are recorded. Cloudy periods are observed on most days. This results in sudden variations in radiation, which, in turn, leads to variations in production. The static methods A1 and PVGIS, therefore, have difficulty making a good prediction. This is not the case with the HPSANFIS method.

Error measures of the mean squared error (MSE), the root mean squared error (RMSE), and the mean absolute percentage error (MAPE) were employed in choosing the best method among candidates. Specifically, the MSE measures an average value of squares of errors, formulated as Eq. (16). Eq. (17) and Eq. (18) give respectively RMSE and MAPE expressions. These results quantify the difference between the predicted and actual output of the plant. The proposed HPSANFIS method has the best performance. It is likely to adapt even to the most extreme conditions of variation, but it has limitations linked mainly to its learning curve and its execution time. The results of the statistical study are shown in Fig.11 and Fig.14. These figures show that, across all seasons (rainy or dry), the proposed model always has the best performance. Performance is also another criterion for the performance of the models. It is given by Eq. (19). It is given for each model and for each season by Fig.12 and 15. These figures show that the proposed model has the highest yield across all

$$MSE = \frac{1}{n} \sum_{i=1}^{n} \left(E_p - E_a \right)^2 \tag{16}$$

$$RMSE = \sqrt{MSE} \tag{17}$$

$$MAPE = 100 * \frac{1}{n} \sum_{i=1}^{n} \left| \frac{E_a - E_p}{E_a} \right|$$
 (18)

$$MAPE = 100 * \frac{1}{n} \sum_{i=1}^{n} \left| \frac{E_a - E_p}{E_a} \right|$$
 (18)

$$Yield (\%) = \frac{E_p}{E_a} * 100$$
 (19)

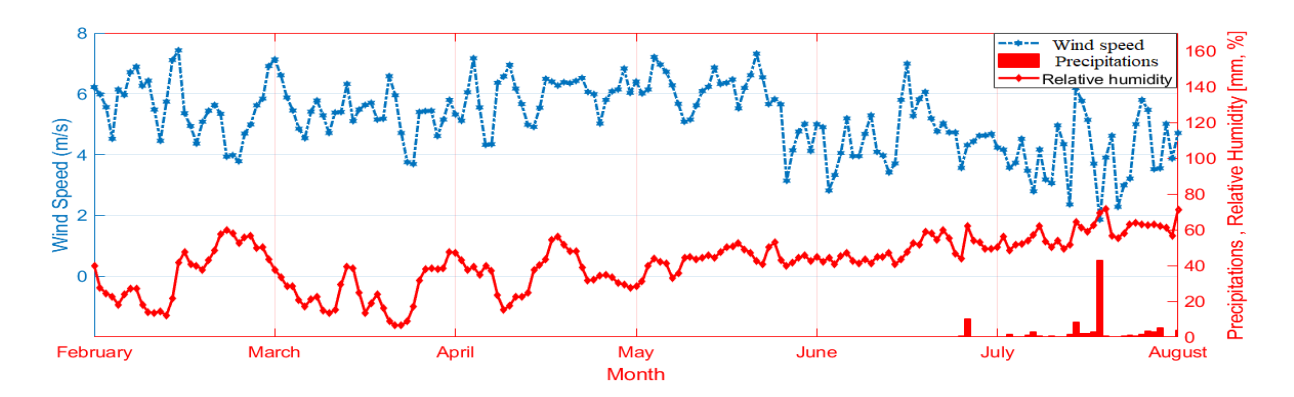


Fig. 9. Evolution of wind speed, relative humidity, and precipitation.

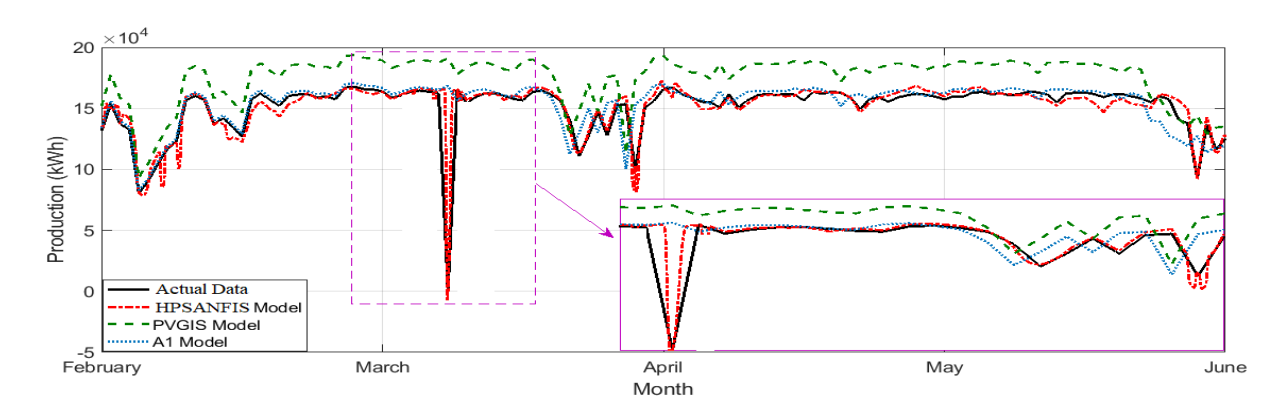


Fig. 10. Production during dry season

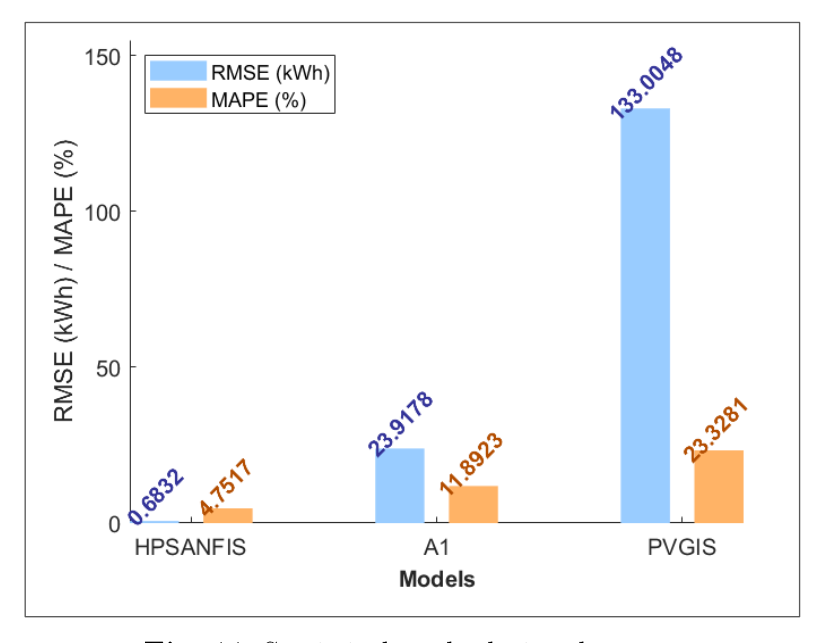


Fig. 11. Statistical study during dry season.

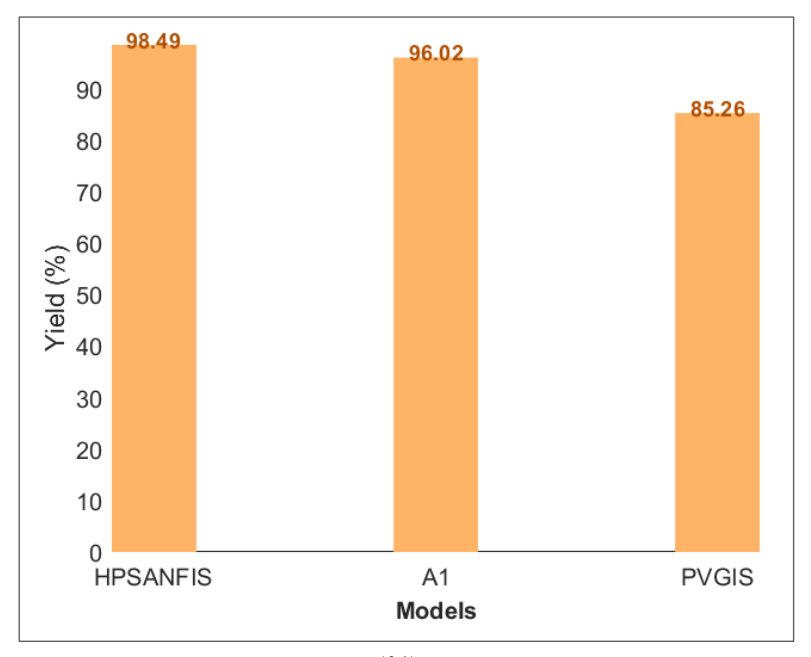


Fig. 12. Model yields (%) during the dry season.

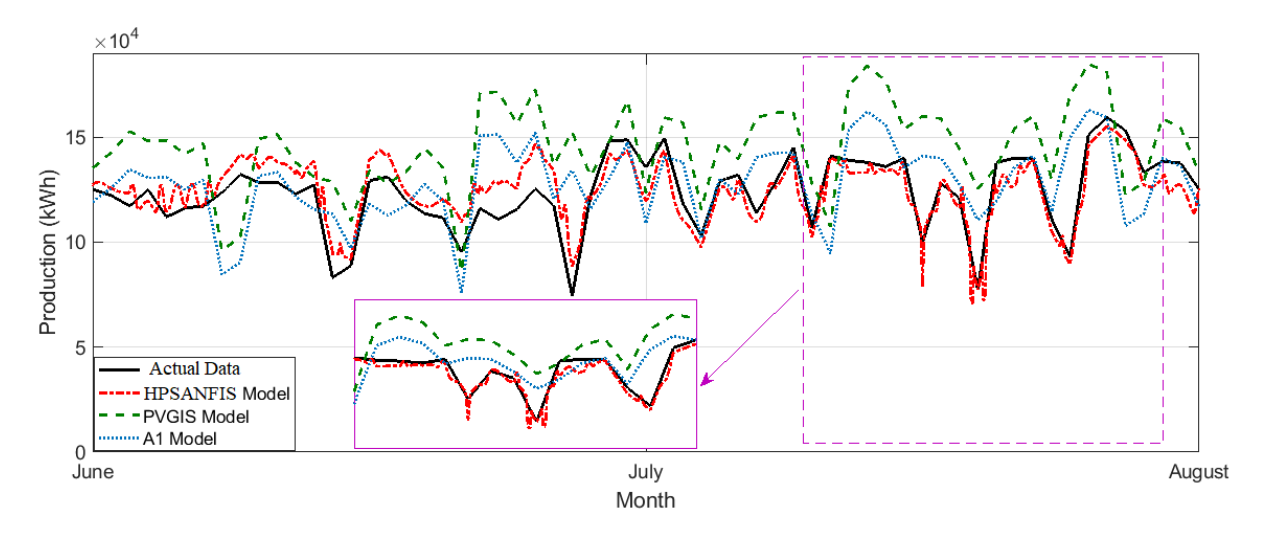


Fig. 13. Production during the rainy season.

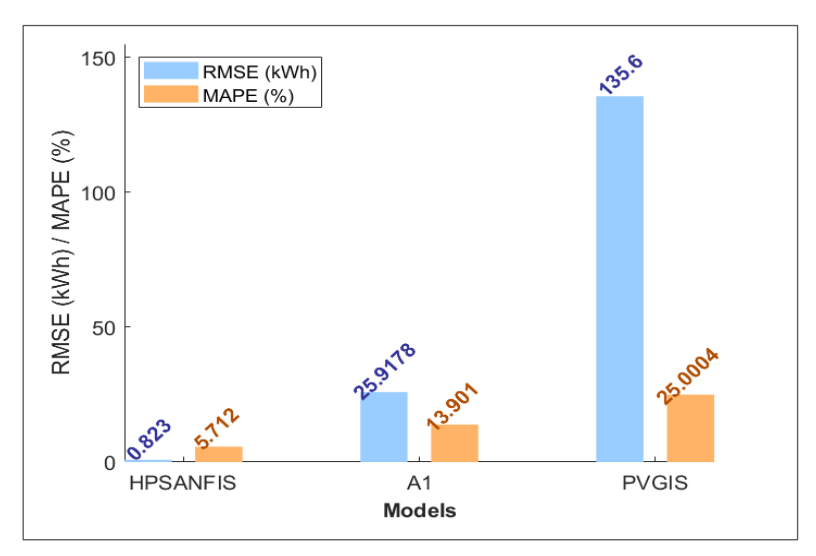


Fig. 14. Statistical study during the rainy season.

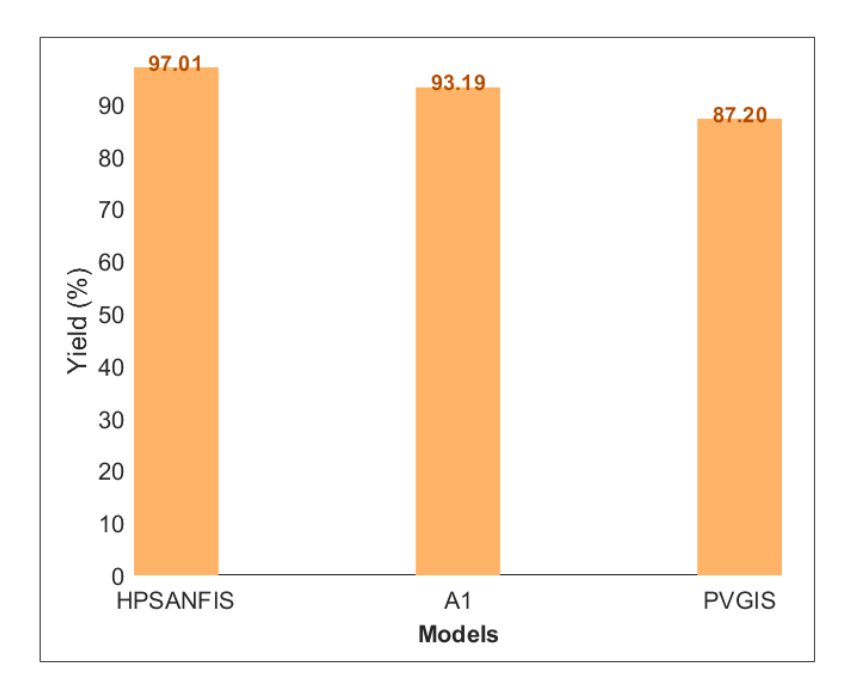


Fig. 15. Model yields (%) during the rainy season.

Significant variations in the plant's output can harm the power grid. The most common consequences are disconnection of the PV system, voltage dips, and bumps. Prediction, therefore, becomes an effective way to manage these problems.

4.5 Discussion

The results obtained in this study superior and confirm the accuracy adaptability of the proposed HPSANFIS hybrid ΑI model for photovoltaic production forecasting at the Ten Merina solar power plants. Beyond predictive metrics, these findings have significant implications for practical and strategic energy management inthe regional context.

From an operational perspective, improved prediction of PV output directly contributes to grid stability. Accurate dayahead and intraday forecasts enable grid operators (such as SENELEC) to anticipate fluctuations, optimize dispatch, and mitigate risks of voltage dips, disconnections, and supply imbalances induced by

renewable variability. The adaptive capacity of the HPSANFIS method, particularly during periods of extreme meteorological variation, supports the integration of large-scale solar PV without undermining grid reliability - a key challenge for African utilities.

On a broader scale, robust solar forecasting is essential for energy transition strategies in Africa. Many African countries, including Senegal, are rapidly increasing their renewable energy share to reduce dependence on fossil fuels and meet sustainability targets. Aspenetration of PVthe unpredictability generation becomes a major barrier to grid expansion and effective market design. The hybrid AI approach demonstrated here can facilitate higher renewable integration by providing accurate, reliable forecasts to support system planning, investment, and real-time operations.

Moreover, the methodology can inform future expansion policies, integrating not only solar but also other intermittent resources (such as wind) within regional energy mixes. By enabling plant owners and grid operators to anticipate production shortfalls and plan appropriate contingencies, the approach also supports consumer-side benefits, including improved service reliability and reduced outage risk. the discussion ofadaptive Finally, forecasting models contributes to global scientific and technical discourse on energy modernization developing system in regions. Future work may extend the present approach to multi-plant aggregation, storage integration, and crosscoordination. border grid further strengthening Africa's capacity for a just and sustainable energy transition.

5 Conclusion

A new method based on evolutionary ANFIS learning with the PSO method was proposed in this paper for forecasting the energy production of Ten Merina solar power plant. The spike and chaotic changes in solar irradiation and PV module temperature series data are used to learn HPSANFIS methodology. methodology is compared with two other methods in the literature: the method used by the PVGIS simulation software and the method based on the performance ratio (A1) method). The specifications of the energy production estimation highlight the necessity of solving a complex task consisting in predicting the Ten Merina solar power plant production system based on the history of production data and weather conditions (availability of solar radiation and PV module temperatures). The proposed HPSANFIS model reliably forecasts PV production across challenging Senegalese seasons, outperforming classical methods. Its adaptability offers utilities and plant operators enhanced planning tools for grid integration and stability. Future work will extend this model to real-time prediction and broader integration of renewable and storage systems.

Acknowledgment

This work was facilitated by the management of the Ten Merina solar power plant. The Laboratory of Water, Energy, Environment and Industrial Processes, ESP, S-10700, Dakar-Fann, Senegal.

References

- [1] E.M. Ndiaye, A. Ndiaye, M. Faye, "Experimental Validation of PSO and Neuro-Fuzzy Soft-Computing Methods for Power Optimization of PV installations," in 8th IEEE International Conference on Smart Grid, (2020) 189–197. doi: 10.1109/icsmartgrid49881.2020.9144790
- [2] A.M. Eltamaly, H.M.H. Farh, M.F. Othman, A novel evaluation index for the photovoltaic maximum power point tracker techniques, Sol. Energy 174 (2018) 940–956. doi: 10.1016/j.solener.2018.09.060
- [3] A. Gligor, C.D. Dumitru, H.S. Grif, Artificial intelligence solution for managing a photovoltaic energy production unit, Procedia Manuf. 22 (2018) 626–633. doi: 10.1016/j.promfg.2018.03.091
- [4] S. Chandra, S. Agrawal, D.S. Chauhan,

 Soft computing based approach to
 evaluate the performance of solar PV
 module considering wind effect in
 laboratory condition, Energy Reports 4
 (2018) 252–259.

doi: 10.1016/j.egyr.2017.11.001

- [5] E. Norouzzadeh, A.A. Ahmad, M. Saeedian, G. Eini, E. Pouresmaeil, Design and implementation of a new algorithm for enhancing MPPT performance in solar cells, Energies 12(3) (2019) 1–17. doi: 10.3390/en12030519
- [6] A.A.S. Mohamed, H. Metwally, A. El-Sayed, S.I. Selem, Predictive neural network based adaptive controller for grid-connected PV systems supplying pulse-load, Sol. Energy 193 (2019) 139–147.
 doi: 10.1016/j.solener.2019.09.018
- [7] A. Ba, A. Ndiaye, E. H. M. Ndiaye, and S. Mbodji, Power optimization of a photovoltaic system with artificial intelligence algorithms over two seasons in tropical area, MethodsX 10 (2023) 101959, 2023, doi: 10.1016/j.mex.2022.101959
- [8] M. Traore et al., Supervision of a PV system with storage connected to the power line and design of a battery protection system, Wirel. Networks (2018). doi: 10.1007/s11276-018-1886-x
- [9] B. Tchanche, Analyse du système énergétique du Sénégal, 21 (2018) 73– 88.
- [10] SENELEC, Rapport Annuel 2018, Senegal (2018).
- [11] P. Mandal, S.T.S. Madhira, A. Ulhaque, J. Meng, R.L. Pineda, Forecasting power output of solar photovoltaic system using wavelet transform and artificial intelligence techniques, Procedia Comput. Sci. 12(915) (2012) 332–337. doi: 10.1016/j.procs.2012.09.080
- [12] J.F. Bermejo, J.F.G. Fernández, R. Pino, A.C. Márquez, A.J.G. López,

- Review and comparison of intelligent optimization modelling techniques for energy forecasting and condition-based maintenance in PV plants, Energies 12(21) (2019) 4163.
- doi: 10.3390/en12214163.
- [13] A. Mbaye, M.L. Ndiaye, J. Ndong, P.A.S. Ndiaye, Impact of Meteorological Parameters on Short-Term Forecasting: Application to the Dakar Site, IEEE 2nd Int. Conf. Power Energy Appl. ICPEA 2010 (2019) 227–231. doi: 10.1109/ICPEA.2019.8818514
- [14] C. Schwingshackl et al., Wind effect on PV module temperature: Analysis of different techniques for an accurate estimation, Energy Procedia 40 (2013) 77–86.
 - doi: 10.1016/j.egypro.2013.08.010
- [15] K.R. Kumar, M.S. Kalavathi, Artificial intelligence based forecast models for predicting solar power generation, Mater. Today Proc. 5(1) (2018) 796– 802. doi: 10.1016/j.matpr.2017.11.149
- [16] M. Diagne, M. David, P. Lauret, J. Boland, N. Schmutz, Review of solar irradiance forecasting methods and a proposition for small-scale insular grids, Renew. Sustain. Energy Rev. 27 (2013) 65–76. doi: 10.1016/j.rser.2013.06.042
- [17] B. Chen, P. Lin, Y. Lai, S. Cheng, Z. Chen, L. Wu, Very-Short-Term Power Prediction for PV Power Plants Using a Simple and Effective RCC-LSTM Model Based on Short Term Multivariate Historical Datasets, Electronics 9(2) (2020) 289. https://doi.org/10.3390/electronics9020289
- [18] A. Bassam, O.M. Tzuc, M.E. Soberanis, L.J. Ricalde, B. Cruz,

Temperature estimation for photovoltaic array using an adaptive neuro fuzzy inference system, Sustainability 9(8) (2017).

doi: 10.3390/su9081399

- [19] A.K. Tossa et al., Artificial intelligence technique for estimating PV modules performance ratio under outdoor operating conditions, J. Renew. Sustain. Energy 10(5) (2018). doi: 10.1063/1.5042217
- [20] W.I. Hameed et al., Prediction of solar irradiance based on artificial neural networks, Inventions 4(3) (2019) 1–10. doi: 10.3390/inventions4030045
- [21] W.M. Nkounga, M.F. Ndiaye, M.L. Ndiaye, O. Cisse, M. Bop, A. Sioutas, Short-term forecasting for solar irradiation based on the multi-layer neural network with the Levenberg-Marquardt algorithm and meteorological data: Application to the Gandon site in Senegal, 7th Int. IEEE Conf. Renew. Energy Res. Appl. ICRERA 5 (2018) 869–874.
- [22] Y.K. Semero, J. Zhang, D. Zheng, S. Member, PV Power Forecasting Using an Integrated GA-PSO-ANFIS Approach and Gaussian Process Regression Based Feature Selection Strategy, CSEE J. POWER ENERGY Syst. 4(2) 210–218. doi: 10.17775/CSEEJPES.2016.01920
- [23] P. Dawan, K. Sriprapha, S. Kittison-tirak, T. Boonraksa, Comparison of Power Output Forecasting on the Inference Systems and Particle Swarm Optimization-Artificial Neural Network Model, Energies 13(2) (2020) 351. doi: 10.3390/en13020351
- [24] J.R. Jang, ANFIS: Adaptive-Network-Based Fuzzy Inference System, IEEE

- 23(3) (1993) 665-685. doi: 10.1109/21.256541
- [25] S. Amirkhani, S. Nasirivatan, A.B. Kasaeian, A. Hajinezhad, ANN and ANFIS models to predict the performance of solar chimney power plants, Renew. Energy 83 (2015) 597–607. doi: 10.1016/j.renene.2015.04.072
- [26] A.A. Aldair, A.A. Obed, A.F. Halihal, Design and implementation of ANFISreference model controller based MPPT using FPGA for photovoltaic system, Renew. Sustain. Energy Rev. 82 (2017) 2202–2217. doi: 10.1016/j.rser.2017.08.071
- [27] S.D. Al-Majidi, M.F. Abbod, H.S. Al-Raweshidy, Design of an efficient maximum power point tracker based on ANFIS using an experimental photovoltaic system data, Electronics 8(8) (2019) 858.

 doi: 10.3390/electronics8080858
- [28] E.M. Ndiaye, A. Ndiaye, M. Faye, S. Gueye, Intelligent Control of a Photovoltaic Generator for Charging and Discharging Battery Using Adaptive Neuro-Fuzzy Inference System, Int. J. Photoenergy 2020(1) (2020) 1-15. doi: 10.1155/2020/8649868
- [29] E.A. Gouda, M.F. Kotb, D.A. Elalfy, Modelling and Performance Analysis for a PV System Based MPPT Using Advanced Techniques, EJECE, Eur. J. Electr. Comput. Eng. 3(1) (2019) 1–7.
- [30] S. Motahhir, A. El Ghzizal, A. Derouich, Modélisation et commande d'un panneau photovoltaïque dans l'environnement PSIM, 2ième édition du Congrès Int. Génie Ind. Manag. des Systèmes (2018) 0–18. doi: https://hal.archives-ouvertes.fr/hal-

01351493

- [31] B. Yang, J. Wang, X. Zhang, M. Zhang, H. Shu, S. Li, MPPT design of centralized thermoelectric generation system using adaptive compass search under non-uniform temperature distribution condition, Energy Convers. Manag. 199 (2019) 111991. doi: 10.1016/j.enconman.2019.111991
- [32] E. Rahma, B. Brahim, M. Smail, A particle swarm optimization-based maximum power point tracking algo-

- $rithm\ for\ PV\ Systems,$ Studies in Engineering and Exact Sciences 5(2) (2024) e11181.
- https://doi.org/10.54021/seesv5n2-577
- [33] O. Ben Belghith, L. Sbita, F. Bettaher, MPPT Design Using PSO Technique for Photovoltaic System Control Comparing to Fuzzy Logic and P&O Controllers, Energy Power Eng. 8(11) (2016) 349–366.

doi: 10.4236/epe.2016.811031